Ultrafast X-Ray Crystallography and Liquidography

Hosung Ki,[1,2] Key Young Oang,[1,2] Jeongho Kim,[3] and Hyotcherl Ihee[1,2]

[1]Department of Chemistry, Korea Advanced Institute of Science and Technology (KAIST), Daejeon 305-701, South Korea; email: kihosung@kaist.ac.kr, wky3219@kaist.ac.kr, hyotcherl.ihee@kaist.ac.kr

[2]Center for Nanomaterials and Chemical Reactions, Institute for Basic Science, Daejeon 305-701, South Korea

[3]Department of Chemistry, Inha University, Incheon 402-751, South Korea; email: jkim5@inha.ac.kr

Annu. Rev. Phys. Chem. 2017. 68:473–97

First published online as a Review in Advance on March 27, 2017

The *Annual Review of Physical Chemistry* is online at physchem.annualreviews.org

https://doi.org/10.1146/annurev-physchem-052516-050851

Keywords

structural dynamics, time-resolved X-ray diffraction, time-resolved X-ray crystallography, serial femtosecond crystallography, time-resolved X-ray liquidography, X-ray free-electron laser

Abstract

Time-resolved X-ray diffraction provides direct information on three-dimensional structures of reacting molecules and thus can be used to elucidate structural dynamics of chemical and biological reactions. In this review, we discuss time-resolved X-ray diffraction on small molecules and proteins with particular emphasis on its application to crystalline (crystallography) and liquid-solution (liquidography) samples. Time-resolved X-ray diffraction has been used to study picosecond and slower dynamics at synchrotrons and can now access even femtosecond dynamics with the recent arrival of X-ray free-electron lasers.

1. INTRODUCTION

XFEL: X-ray free-electron laser

Chemical reactions are dynamic processes whereby reactants transform into products with changes in molecular structures and energies. The ultimate goal of reaction dynamics studies is to understand how the constituent atoms in reacting molecules rearrange their chemical connectivity during a chemical reaction, that is, the reaction mechanism. To achieve this goal, it is desirable to monitor the progress of a reaction over time and, accordingly, various time-resolved methods have been developed over many decades (1–9). Among them, time-resolved optical spectroscopy has served as a major tool for elucidating the dynamics and mechanisms of chemical and biological reactions. Time-resolved optical spectroscopic techniques make use of multiple laser pulses at optical wavelengths and generally employ a pump–probe scheme, where an optical (pump) pulse is used to initiate a photochemical reaction and a time-delayed, optical (probe) pulse is used to monitor the progress of the reaction. With the technical advances of laser technology, femtosecond laser pulses can be readily generated from tabletop lasers, and it has become possible to monitor chemical dynamics with ultrafast temporal resolution using time-resolved optical spectroscopy. In addition, time-resolved optical spectroscopy is a highly selective and sensitive technique for monitoring the dynamics of molecular processes because specific molecular states can be selectively excited and probed by varying the wavelengths and polarizations of the pump and probe pulses. However, the optical spectroscopic signals are not directly related to the global molecular structure; therefore, to obtain the time-dependent structural change of reacting molecules, it is necessary to perform extensive theoretical analysis of time-resolved spectroscopic data, which is quite difficult, or even impossible, for large molecular systems.

As a means of addressing this limitation of optical spectroscopy, time-resolved X-ray diffraction (or scattering) has been developed. In time-resolved X-ray diffraction, an X-ray pulse is used as the probe pulse in the pump–probe scheme. Because X-rays are diffracted (or scattered) off all atomic pairs present in the sample molecules, structural information of reacting molecules can be directly retrieved from time-resolved diffraction patterns measured by varying the pump–probe time delay. Through technical advances of analytical tools, time-resolved X-ray diffraction has become applicable to samples not only in the solid crystalline phase but also in the liquid and solution phases. More importantly, the recent development of X-ray free-electron lasers (XFELs) has substantially improved the temporal resolution of time-resolved X-ray diffraction, which now has superb resolution in both time and space domains. In this review, we discuss the applications of time-resolved X-ray diffraction to the investigation of chemical and biological reactions in the crystalline and solution phases.

2. TIME-RESOLVED X-RAY DIFFRACTION

In general, a chemical reaction involves multiple reaction pathways. To have a complete understanding of the reaction dynamics, it is desirable to elucidate the reaction rates and branching ratios of all the reaction pathways. In this regard, time-resolved X-ray diffraction has several advantages over time-resolved optical spectroscopy. First, the X-ray diffraction pattern of a given molecule can be calculated accurately using a rather simple equation as long as the structure of the molecule is known or can be predicted. In contrast, the calculation of the electronic spectrum of a given molecule is complicated and often inaccurate, especially for large molecules (10, 11). Therefore, compared with time-resolved optical spectroscopy, it is more straightforward to explain the molecular origin of a time-resolved X-ray diffraction signal by theoretical tools. Second, in addition to the direct relationship between the molecular structure and the X-ray diffraction signal, the molecular structure can be predicted with high accuracy, even with low-cost quantum

calculations, whereas the energy calculation of excited states requires high-level calculations but is often still inaccurate (11, 12). Third, most importantly, time-resolved X-ray diffraction is equally sensitive to all species formed during a reaction because the diffraction signal consists of contributions from all the reaction species. In contrast, time-resolved optical spectroscopy is sensitive only to specific species that have high oscillator strengths at given probe wavelengths. Therefore, in principle, X-ray diffraction can probe all the species involved in the reaction without missing any spectroscopically dark states. In this way, not only can the reaction species be identified, but their relative fractions can be accurately determined from X-ray diffraction intensities. In other words, time-resolved X-ray diffraction can directly visualize global reaction pathways and is thus an excellent tool for studying chemical reaction dynamics. These advantages of time-resolved X-ray diffraction, however, represent only one side of a coin. Because X-ray diffraction can detect all the chemical species present in a sample, even including the solvent molecules in solution samples, it has lower selectivity than optical spectroscopy. For example, by tuning the probe wavelength, time-resolved optical spectroscopy can selectively probe a certain species of interest, allowing it to detect even a species of extremely low concentration. In contrast, the contribution of each species to a time-resolved X-ray diffraction signal is proportional to its concentration, and therefore the contributions of minor species can be obscured by those of major species.

In this review, we classify time-resolved X-ray diffraction techniques by three criteria schematically shown in **Figure 1**:

- phase of target molecules (crystallography versus liquidography);
- size of target molecules (small molecules versus macromolecules); and

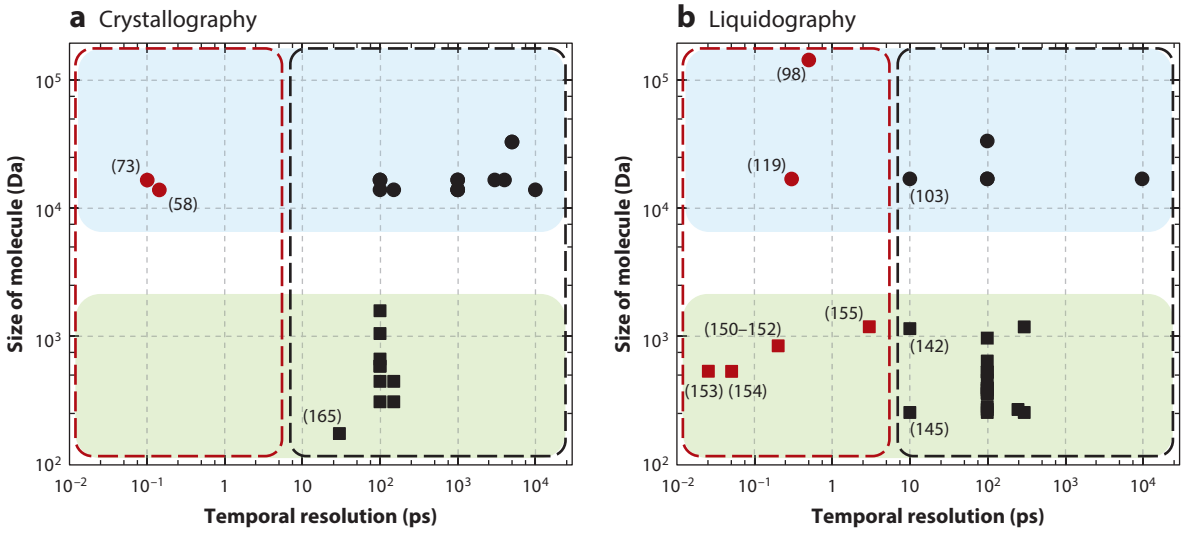

Figure 1

A scatter plot showing the distribution of previous studies using (*a*) time-resolved X-ray crystallography and (*b*) time-resolved X-ray liquidography with respect to the temporal resolution of the experiment and the size of its target molecules. Only studies on small molecules and proteins are depicted. Each symbol represents a study. The shape of each symbol represents the size of the sample molecules used for the study (*circle*: protein; *square*: small molecule). The color of symbols denotes the source of X-ray pulses used for each study (*black*: synchrotron; *red*: X-ray free-electron laser). To avoid ambiguity, the shortest positive time delay measured in an experiment is regarded as the experiment's temporal resolution. The reference numbers for representative studies (58, 73, 98, 103, 119, 142, 145, 150–155, 165) are displayed next to their corresponding symbols.

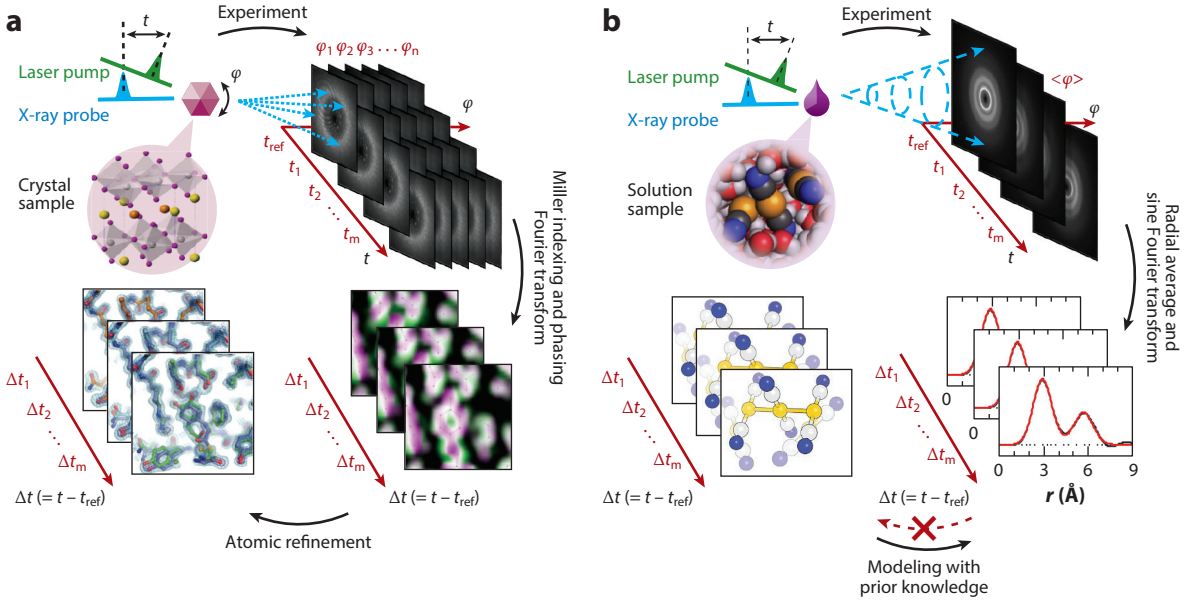

Figure 2

Comparison of X-ray crystallography and X-ray liquidography. (*a*) Diffraction from regular arrays of molecules in a single crystal produces strong Bragg spots. The Bragg spots are collected at multiple orientations of the crystal and indexed to fully span the three-dimensional diffraction intensities in reciprocal *q*-space. After retrieving phase information, the three-dimensional diffraction intensities can be directly converted to a three-dimensional electron density distribution using a Fourier transform. Further refinement using atomic models results in a high-resolution, three-dimensional structure. (*b*) Scattering from randomly oriented molecules in solution yields smooth, centrosymmetric scattering patterns. The orientation-averaged pattern lacks the scattering intensities in three-dimensional reciprocal space and instead contains only the scattering intensities in one-dimensional *q*-space. The one-dimensional scattering intensities can be converted to a one-dimensional pair distance distribution in real space, which is not in one-to-one correspondence with a three-dimensional structure. Therefore, a modeling approach based on prior knowledge is required to retrieve a unique three-dimensional structure from the pair distance distribution.

- temporal resolution of time-resolved X-ray diffraction dictated by the X-ray source (synchrotron versus XFEL).

With respect to the first criterion, depending on the phase of a sample used for measurement, time-resolved X-ray diffraction is called either time-resolved X-ray crystallography (TRXC), when applied to solid crystalline samples, or time-resolved X-ray liquidography (TRXL) [or time-resolved X-ray solution scattering (TRXSS)], when applied to liquid or solution samples (see **Figure 2**). A simple comparison between TRXC and TRXL is given in **Table 1**. Because of the difference in the sample phase, X-ray diffraction patterns obtained by the two techniques are of different characters and have different spatial resolutions. The diffraction from ordered arrays of molecules in crystals yields intense Bragg spots, which can be directly converted to a three-dimensional (3D) structure with atomic resolution. Thus, crystallography has been the most powerful tool for characterizing molecular structure. In contrast, the scattering from randomly oriented molecules in the liquid and solution phases yields smooth centrosymmetric patterns. These orientation-averaged patterns can be converted to only one-dimensional (1D) atomic-pair distance distributions in real space. Therefore, the conversion of the solution scattering pattern to a 3D structure requires a modeling approach, whereby a theoretical scattering pattern calculated from a 3D model structure is compared with the experimental scattering pattern and the model structure is optimized until the

TRXC: time-resolved X-ray crystallography

TRXL: time-resolved X-ray liquidography

TRXSS: time-resolved X-ray solution scattering

Table 1 Comparison of TRXL and TRXC

	TRXL		TRXC	
	Small molecules	**Proteins**	**Small molecules**	**Proteins**
Sample environment	Solvated; randomly oriented (some photoselective alignment is possible); unequally spaced		Densely packed	Loosely packed
			Uniformly oriented; equally spaced	
Obtained signal	Centrosymmetric rings (some degree of anisotropic scattering is possible)		Bragg spots	
Sample delivery	Liquid jet	Closed capillary or flow cell	Crystal loop (low temperature); capillary (room temperature); jets or fixed target for SFX	
Sample limitations	Soluble molecules or proteins		Crystallizable molecules or proteins	
Required coverage of scattering angles	Wide (at least 3 $Å^{-1}$ and typically more than 6 $Å^{-1}$)	Small (less than 1 $Å^{-1}$)	Wide (typically more than 6 $Å^{-1}$)	Medium (typically ~2–4 $Å^{-1}$)
Structural analysis	Modeling approach		Direct retrieval (electron density); refinement of atomic structure	
Spatial resolution	Medium (near atomic structural changes)	Limited (large conformational changes or helices movements for well-defined rigid structure)	High (atomic structural changes)	High (atomic structural changes)
Temporal resolution	~100 ps (synchrotron); <1 ps (XFEL)			

Abbreviations: SFX, serial femtosecond crystallography; TRXC, time-resolved X-ray crystallography; TRXL, time-resolved X-ray liquidography; XFEL, X-ray free-electron laser.

theoretical and experimental scattering patterns match each other. As a result, TRXL has a lower spatial resolution than TRXC.

With respect to the second criterion, depending on the size of the target molecules, different approaches to experiment and data analysis should be taken, especially for TRXL applied to solution samples. Small molecules and proteins are two representative groups of target systems that have been studied using time-resolved X-ray diffraction because of their importance in chemistry and biology. When performing TRXL experiments, the experimental conditions, such as the range of scattering angles and the sample delivery system, are very different for small molecules and proteins. Also, the data analysis approach for TRXL is quite different for small molecules and proteins. For small molecules, the data analysis aims to obtain detailed changes in molecular structure at the atomic level. In contrast, for proteins, the data analysis aims to extract only large-scale changes of global conformation, mainly because of the inherently limited spatial resolution of TRXL. Although a variety of large systems, such as metal nanoparticles (13, 14), nanowires (15), metal thin films (16), and DNAs (17), have also been studied using time-resolved X-ray diffraction, only studies on small molecules and proteins are covered in this review (see **Figure 1**).

With respect to the third criterion, depending on the X-ray source, the temporal resolution of time-resolved X-ray diffraction varies significantly. Because femtosecond optical laser pulses are readily available, the temporal resolution of time-resolved X-ray diffraction is commonly dictated by the temporal duration of X-ray (probe) pulses used for the experiment. When time-resolved X-ray diffraction experiments are performed at third-generation synchrotrons, a temporal resolution of ~100 ps is obtained. Although the time-slicing approach was developed to improve this temporal resolution, it is still difficult to study ultrafast reactions occurring on subpicosecond timescales at synchrotrons. Recently, the arrival of XFEL sources has improved the temporal

resolution of time-resolved X-ray diffraction experiments down to the femtosecond timescale (see **Figure 1**), making the technique more powerful.

SFX: serial femtosecond crystallography

3. TIME-RESOLVED X-RAY CRYSTALLOGRAPHY FOR MACROMOLECULES

In the middle of the twentieth century, it was demonstrated that the complex structure of macromolecules, even ones consisting of tens of thousands of atoms, can be characterized using X-ray crystallography (18). Since that success, X-ray crystallography has served as a workhorse tool for characterizing the structures of biological macromolecules, for example, proteins. Researchers have recently realized that, for a better understanding of the mechanism of protein functions, the dynamic structure of a protein that evolves during its structural transition is more relevant to investigate than its static structure. Accordingly, TRXC was proposed (1, 19, 20) and developed (21, 22) as a tool for investigating the structural dynamics of protein transitions.

For TRXC studies of protein crystals, the Laue crystallography method has been mainly used. Laue crystallography utilizes Laue diffraction patterns obtained by the diffraction of intense polychromatic X-rays off protein crystals and has many advantages (23) over monochromatic X-ray diffraction techniques. A time-resolved difference electron density map measured by TRXC is an intricate mixture of many dynamic structures. To retrieve the structures and transition kinetics of various reaction intermediates from the TRXC data, it is necessary to perform kinetic analysis for a series of time-resolved density maps measured at various time delays. Such analysis is facilitated by applying a mathematical method called singular value decomposition (SVD) (24) to the crystallographic data (25). Subsequent analysis of the singular vectors obtained from the SVD analysis provides the structures and kinetics of the intermediate species simultaneously. The procedure of SVD-based analysis is described in detail in the literature (25, 26).

Although TRXC has served as a powerful tool for elucidating structural dynamics of macromolecules (27–31), its application has been limited to only a few proteins for several technical reasons. First, X-ray crystallography requires well-diffracting protein crystals, but it is often difficult or impossible to prepare sizable protein crystals. Second, for experimenters to collect data with a sufficiently high signal-to-noise ratio (SNR) within a limited beam time, a protein transition needs to be readily reversible, that is, the photoexcited protein returns to its initial ground state in a reasonably short time (at most a few seconds). Third, a protein crystal should be reasonably strong against X-ray radiation, so that diffraction images of decent SNR can be measured at various time delays and at all needed crystal orientations without significant radiation damage. Because of these requirements, TRXC has been applied to only a few model proteins that undergo reversible photoinduced transitions, for example, photoactive yellow protein (PYP) (26–28, 31–35), homodimeric hemoglobin (36, 37), and myoglobin (29, 38–43). Excellent reviews on the TRXC studies of protein dynamics were presented by Bourgeois & Royant (44), Neutze et al. (45), and Moffat (46).

Recent development and operation of a new X-ray source, XFELs, has been a breakthrough for X-ray crystallography. By fully making use of the ultrashort, intense X-ray pulses generated by XFELs, researchers devised a new scheme for X-ray crystallography called serial femtosecond crystallography (SFX) (47–50). In this novel experimental scheme, each diffraction image is obtained with a single femtosecond X-ray pulse diffracted off a fresh crystal of protein. This single-shot diffraction scheme minimizes radiation damage because the femtosecond X-ray pulse interacts with the crystal for only a brief moment and is diffracted before the protein crystal is damaged by the X-ray radiation. Thanks to the extreme brightness of the X-ray pulse from an XFEL, the diffraction intensity is still large enough to give a diffraction image with a high SNR. A protein crystal exposed to a single X-ray pulse is disposed of because it can be damaged significantly

after even a single interaction with the intense X-ray pulse from an XFEL (51). To fully span the diffraction intensities in the reciprocal space, this single-shot measurement is repeated hundreds of thousands of times, and such repeated measurements for different, fresh crystals are why this experimental scheme is said to be serial. The static structure of a protein can be determined by SFX with minimal radiation damage (47, 52–55). Also, when the SFX technique is combined with an optical pump pulse to initiate the photoinduced transition, it can be implemented in a time-resolved manner so that the structures of short-lived transient intermediates formed during the protein transition can be captured (56–59).

TRSFX: time-resolved serial femtosecond crystallography

Conical intersection: the point in nuclear coordination space where adiabatic electronic potential energy surfaces are degenerate

It was recently demonstrated that time-resolved serial femtosecond crystallography (TRSFX) can serve as an excellent tool for probing structural dynamics of protein transitions, with several advantages over conventional TRXC based on the Laue method (56, 58–61). First, nano-to-microcrystals can serve as excellent samples for TRSFX, whereas they are considered too small for the time-resolved Laue crystallography performed at synchrotrons (47). Such small crystals are often observed during the crystallization process that leads to the formation of macrocrystals and are believed to be much easier to prepare than macrocrystals (62–65), although there is some debate (66). In addition, the small crystals generally have fewer defects than larger crystals. Thus, TRSFX has great potential to be applied to more diverse proteins than conventional TRXC, especially to proteins that are difficult to crystallize in large size. Second, TRSFX can determine the transient structures of a protein without the effect of X-ray radiation damage, as expected from the principle of SFX and supported by theoretical studies (51, 67). The lack of X-ray radiation damage is particularly important for some proteins that are very vulnerable to such damage (68–71). Third, most importantly, TRSFX can be implemented with femtosecond temporal resolution when combined with femtosecond optical pump pulses. In general, large-amplitude conformational change of a photoactive protein is triggered by a small structural change in an organic chromophore (72). To completely understand the mechanism of a protein structural transition, it is important to reveal the underlying connection between the local structural change of residues surrounding the chromophore and the global conformational change of the entire protein matrix. Because the initial structural change of the chromophore often occurs very fast, even down to tens of femtoseconds, the achievement of femtosecond temporal resolution by TRSFX is a major breakthrough that will allow us to capture the earliest events of protein transitions.

Femtosecond TRSFX study of protein dynamics was first demonstrated by Schlichting and coworkers (73). In that work, ultrafast structural changes in CO-bound myoglobin (MbCO) were directly observed with subpicosecond resolution. In particular, the detailed motions of amino acid residues and the heme chromophore within 500 fs after CO dissociation were clearly visualized (see **Figure 3**). Interestingly, collective movements of residues around the heme exhibit an oscillatory feature. The coherent oscillatory motions indicate strong coupling between the dissociation of the CO ligand and the collective motions of surrounding residues. Later, Schmidt and coworkers (58) used femtosecond TRSFX to probe the earliest events of the photocycle of PYP. In that work, the structural changes associated with the *trans*-to-*cis* isomerization of the chromophore were clearly visualized (see **Figure 4**). In particular, it was found that, at ~550 fs, the isomerization of the PYP chromophore passes through a conical intersection between the electronically excited state and the ground state.

Besides these advantages of TRSFX over conventional TRXC, the serial nature of TRSFX is expected to lead to another significant breakthrough for TRXC. Previously, the application of conventional Laue-type TRXC was limited to reversible protein transitions because measurement on irreversible protein transitions would require too much time and sample. However, the investigation of irreversible protein transitions is inherently allowed by the serial nature of the TRSFX scheme, whereby a fresh crystal is provided for each pair of laser and X-ray pulses. In addition,

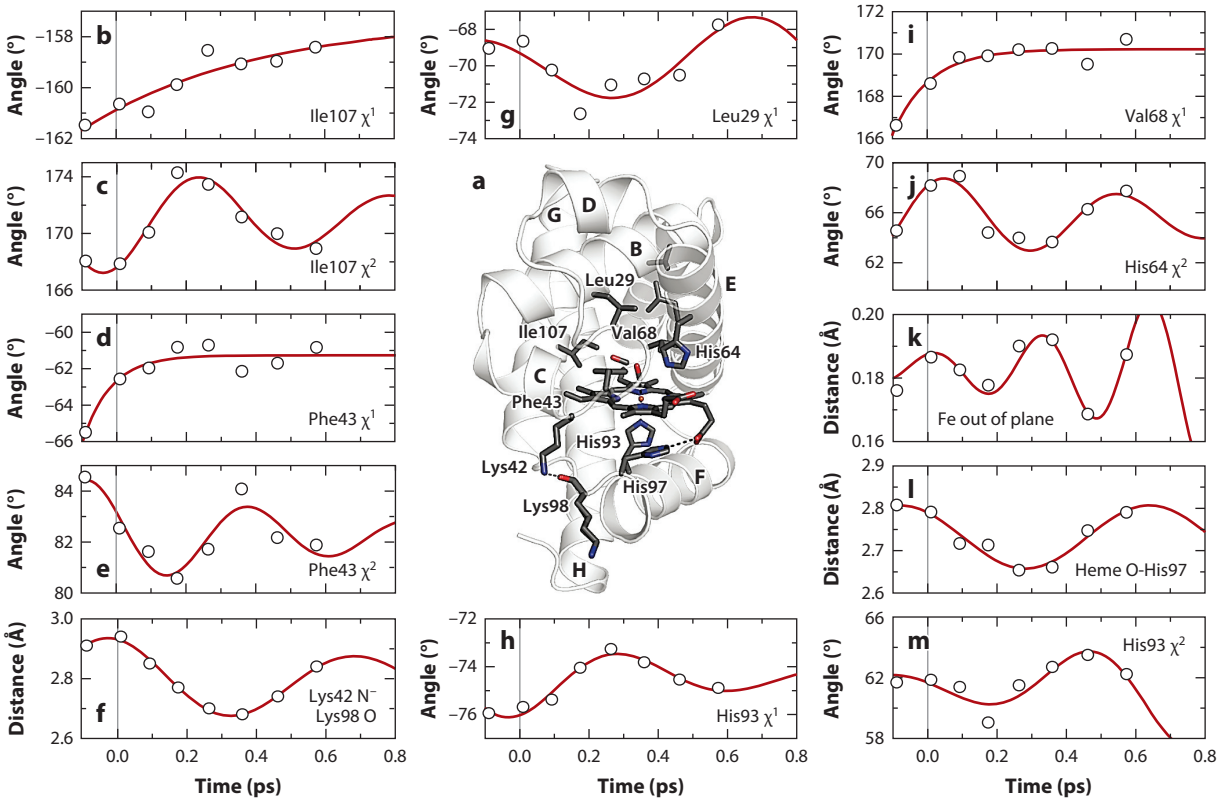

Figure 3

Ultrafast collective motions of residues around the heme chromophore in CO-bound myoglobin observed using femtosecond time-resolved serial femtosecond crystallography (73). (*a*) The ground-state structure of CO-bound myoglobin. The heme chromophore and surrounding residues exhibiting ultrafast motions are displayed using sticks. (*b–m*) Ultrafast structural fluctuation of the chromophore and the residues displayed in panel *a*. For each residue, data points showing the time dependence of a structural parameter are plotted as empty circles, and their theoretical fit with a damped oscillation or a single exponential is displayed as a red line.

TRSFX provides the opportunity of going beyond structural transitions of photoactive proteins. For example, photocaged molecules, which release molecules trapped inside the cage upon photoexcitation, can be used to synchronize diffusion-controlled reactions of macromolecules that are inactive to photoexcitation. Previously, it was demonstrated with a conventional TRXC experiment that a substrate–enzyme reaction can be triggered with photoexcitation of a caged substrate bound to an enzyme (21, 74–77). Thus, the targets of the TRXC technique are no longer limited to a few model systems that undergo reversible photocycles but now include a wide variety of biologically meaningful macromolecules.

4. TIME-RESOLVED X-RAY CRYSTALLOGRAPHY FOR SMALL MOLECULES

TRXC can also be applied to small molecules, as X-ray crystallography is presumably the most effective method for determining molecular structure, irrespective of the size of molecules. However, the crystallography is implemented quite differently for small molecules and

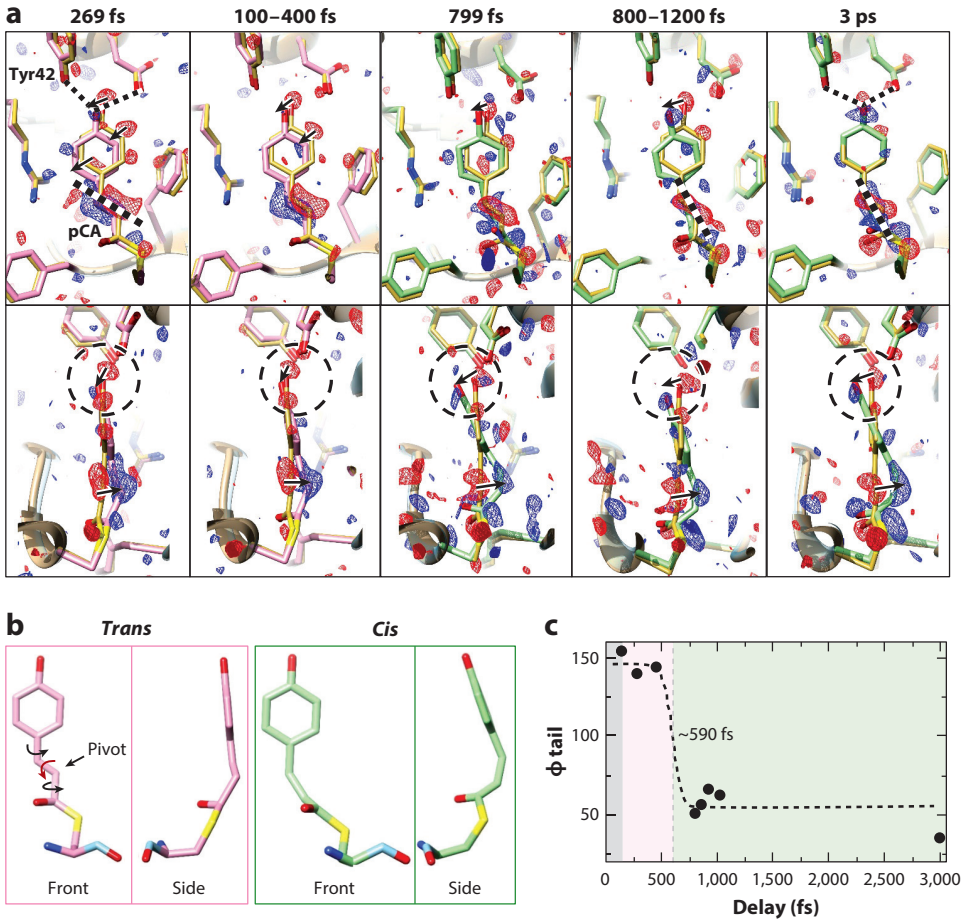

Figure 4

Ultrafast structural dynamics of the chromophore in photoactive yellow protein (PYP) captured using femtosecond time-resolved serial femtosecond crystallography (58). (*a*) Weighted difference electron density (DED) maps around the PYP chromophore in red (-3σ) and blue (3σ), shown in front view (*top*) and side view (*bottom*), where σ indicates one standard deviation of the DED. The time-dependent DED maps clearly show the progress of *trans*-to-*cis* isomerization of the pCA chromophore. The reference dark structure, the structure before the transition, and the structure after the transition are shown in yellow, pink, and light green, respectively. (*b*) Structures of the *trans* (*left*) and *cis* (*right*) isomers of the chromophore; front view (*left*, within each of *cis* and *trans*) and side view (*right*, within each of *cis* and *trans*). (*c*) Dynamics of the torsional angle φ_{tail} of the chromophore tail. The theoretical fit with a 590-fs transition time is presented as a dashed line. Pink and light green regions correspond to the times before and after the transition. The gray region is the time that was not probed by the experiment.

macromolecules because of the different natures of their crystals. The crystals of small molecules are of much higher quality than those of macromolecules, for example, because the small molecules are more regularly ordered and more densely packed in the crystal. The high-quality crystals of small molecules produce strong Bragg diffraction spots up to high orders, which produce molecular structures at subatomic resolution. The phase can be routinely obtained using a direct method, and structural refinement is simple because of the small number of atoms

constituting the small molecules. From the viewpoint of dynamics, however, reactions in the crystals of small molecules are highly constrained (78–80) because the constituent molecules are packed densely and strongly, in contrast to macromolecules, which are loosely packed and often surrounded by a large number of solvent molecules in the crystalline phase.

At the beginning of TRXC experiments for small molecules, monochromatic X-ray pulses were used as probes in order to obtain high-resolution molecular structures at atomic or subatomic levels (78). To compensate for the low intensity of monochromatic X-ray pulses, the sample, excited by a short optical laser pulse, was immediately exposed to a long train of X-ray pulses (up to tens of microseconds after excitation by the laser pulse) and the pump–probe cycle was rapidly repeated (at a frequency of up to several kilohertz) (81, 82). Because of the rapid repetition, this type of TRXC method is not applicable to irreversible reactions or molecular crystals that are easily damaged by laser and X-ray radiation. This method has been applied to photoinduced reactions of various molecular crystals, including diplatinum complex (82), copper phenanthroline (83, 84), copper pyrazolate trimer (85), dirhodium complex (86), iron complex (87), and electron-transfer organic molecules (88).

However, TRXC using monochromatic radiation was subject to a number of major limitations, such as serious radiation damage of the sample, limited access to processes with slow recovery times, and inability to access processes faster than the duration of a long X-ray pulse train. As a means of overcoming these limitations, intense, polychromatic X-rays can be used as a structural probe of molecular crystals, as already demonstrated for time-resolved Laue crystallography of proteins. With the development of a new analytic method (89), the Laue method can resolve even very small changes of atomic positions in molecular crystals. Consequently, the time-resolved Laue method has been applied to various photoreactions of small molecules, including bridged dirhodium complex (78, 90), spin-crossover iron complex (91), silver–copper tetranuclear complex (92), and copper phenanthroline complex (93). As time-resolved Laue crystallography has been applied to molecular crystals successfully, it has become possible to probe processes as fast as the subnanosecond timescale with atomic spatial resolution. Most TRXC studies on small molecules have been done by Coppens and coworkers, who published an excellent review on this topic (94).

The TRXC technique has not yet been applied to molecular crystals at XFELs. Instead, there have been a number of studies by Miller and coworkers (95, 96) on the reactions of molecular crystals using ultrafast electron diffraction. However, the method of retrieving the molecular structures used in these electron diffraction studies was significantly different from the one used for X-ray crystallography. With ultrafast electron diffraction, the diffraction intensities were measured only from a few selected orientations of the crystal, and therefore the diffraction amplitudes were sampled for only a part of reciprocal space, which is not enough to reconstruct an electron density map via a Fourier transform. To retrieve a molecular structure from such limited information, the diffraction intensities were fitted by theoretical intensities calculated from model structures, a method that resembles the data analysis strategy used for TRXL.

It is worthwhile to note that the TRXC methods using either monochromatic or polychromatic X-rays at synchrotrons are suitable for rapidly reversible reactions in crystals but inadequate for irreversible reactions or reversible reactions with very slow recovery time. To gain access to the structure of intermediate species in such irreversible reactions, the scheme of TRSFX can be adapted to molecular crystals. The feasibility of TRSFX has already been demonstrated for proteins (47, 52, 59, 71). By employing the serial concept of SFX, it is expected that ultrafast dynamics of irreversible reactions occurring in molecular crystals can also be accessed using TRXC.

5. TIME-RESOLVED X-RAY LIQUIDOGRAPHY FOR MACROMOLECULES

Although TRXC has served as an excellent tool for investigating the structural dynamics of macromolecules, it has two major drawbacks. First, TRXC is only applicable to proteins that can be crystallized. Second, the structural dynamics probed by TRXC occur in the crystalline phase and might be different from those occurring in the aqueous phase, which is the physiological condition of living organisms. For example, large conformational changes such as protein folding/unfolding can destroy the crystalline lattice or be restricted by crystal packing in the crystalline phase. Because most biological functions of living organisms are performed in the solution phase, it is desirable to observe the structural changes of proteins in solution. In this regard, TRXL is relevant for observing the motions of proteins in their physiological conditions.

However, the visualization of the reaction dynamics in solution is not as straightforward as for reactions in the crystalline phase because molecules in solution are unequally spaced and randomly oriented. As a result, centrosymmetric scattering patterns, not Bragg spots, are obtained from solution samples, and therefore TRXL has inherently lower spatial resolution than TRXC. For large macromolecules such as proteins, it is not practically possible to elucidate all the atomic-level details of structural changes using TRXL. In addition, in the solution phase, a solute molecule of interest is surrounded by a much larger number of solvent molecules, most of which do not directly participate in the reaction, and the solution scattering pattern is dominated by the contributions of solvent molecules. To minimize the solvent contribution, difference scattering curves are obtained in the TRXL measurement by taking the difference between scattering curves measured before and after initiating the reaction, $\Delta S(q) = S(q)_{\text{pump on}} - S(q)_{\text{pump off}}$. Once a series of time-resolved difference scattering curves are measured at various time delays, they can be kinetically analyzed using SVD and principal component analysis to extract (*a*) species-associated difference scattering curves, which are characteristic of the structures of reaction intermediates, and (*b*) time-dependent concentrations of the reaction intermediates (97–104). In general, the formation of reaction intermediates of a protein structural transition accompanies large-amplitude changes of global conformation of the protein. Therefore, from kinetic analysis, the dynamics of conformational changes of proteins can be revealed by TRXL. Also, with the aid of structural refinement methods such as rigid-body modeling, the detailed motions of secondary structural elements (for example, α-helices) can be retrieved from the TRXL data. The experimental scheme and data analysis of TRXL are described in detail in the literature (3, 105–108).

Previous TRXL studies on several model proteins in the solution phase performed at synchrotrons demonstrated that molecular movies of proteins in the solution phase can be filmed using TRXL, as described in a recent review (109). In particular, TRXL has elucidated the structural dynamics of various heme proteins, such as hemoglobin (Hb) (110), myoglobin (Mb) (102, 103, 111–113), and homodimeric hemoglobin (97, 104). For example, TRXL was used to investigate the structural changes of Hb related with its function, that is, the R-T transition that occurs with uptake or release of small ligand molecules (110). That study revealed the dynamics of tertiary and quaternary structural changes of Hb related to its R-T transition and is the first case of probing the structural dynamics of proteins in the solution phase using time-resolved X-ray diffraction. For Mb, TRXL studies elucidated the details of tertiary structural changes (111) and comprehensive structural dynamics (102, 113) down to a timescale of less than 100 ps (103). In addition, anisotropic scattering patterns measured from transiently aligned Mb molecules by linearly polarized photoexcitation were analyzed to determine the rotational diffusion time (~15 ns) of the protein (114).

Besides the heme proteins, TRXL has been used to investigate structural dynamics of various proteins, for example, bacteriorhodopsin and proteorhodopsin (115), which are light-driven proton pumps in membranes; PYP (100, 116, 117) and phytochrome (99), which are photosensory proteins; and cytochrome c (Cyt c) (101, 110), which is a heme protein involved in the electron transport chain in mitochondria. Among these examples, the TRXL studies of Cyt c clearly show the advantage of TRXL over TRXC (110). Cyt c has served as a good model system for studying folding and unfolding processes of proteins. The folding and unfolding processes of a protein cannot be probed by TRXC because (*a*) they destroy the crystalline lattice due to large conformational changes and (*b*) the unfolded proteins cannot be crystallized due to their flexible nature. In contrast, TRXL can readily probe large conformational changes of proteins, even for flexible proteins (118), as demonstrated by TRXL studies on the folding process of Cyt c (101, 110).

As was the case for TRXC, femtosecond X-ray pulses introduced by an XFEL can improve the temporal resolution of TRXL down to hundreds of femtoseconds, allowing us to investigate the initial steps of photoinduced reactions of proteins in solution. Two successful cases were recently demonstrated by Neutze and coworkers (98) and Cammarata and coworkers (119). Using femtosecond TRXL, Neutze and coworkers studied the photoinduced structural transition of the photosynthetic reaction center, which performs the primary energy conversion reactions of photosynthesis. In spectroscopic studies, it had been suggested that the primary charge separation reactions in this complex would accompany ultrafast structural change (120–123). From the femtosecond TRXL experiment on the reaction center performed by Neutze and coworkers (98) using XFEL technology, the dynamics of structural deformation were captured on a subpicosecond timescale. In particular, it was revealed that the structural deformation of the reaction center is initially localized at the chromophore and propagates to a domain of the complex over time. This observation is valuable as the first direct structural evidence of the protein quake in solution (124, 125), a rapid propagation of light-induced structural deformation through a protein via a quake-like intramolecular motion.

Cammarata and coworkers (119) used TRXL at an XFEL to unveil the initial stage of the photolysis of MbCO in solution (see **Figure 5**). Time-resolved X-ray scattering curves were measured with subpicosecond temporal resolution (see **Figure 5*a***) and analyzed to provide time-dependent structural parameters of proteins, for example, the radius of gyration (R_g) and the volume of protein (V_p) (see **Figure 5*b***). Notably, the time evolution of those structural parameters reveals an oscillatory collective motion of constituent atoms of Mb, especially significant within 10 ps. Based on the oscillatory collective motion, the authors postulated an intrinsic ballistic-like nature of protein motion (see **Figure 5*d***) that is generally hidden in ensemble measurements on longer timescales.

These two results demonstrate the capability of TRXL as a tool for investigating the structural dynamics of proteins. Owing to the excellent structural sensitivity of X-ray solution scattering and the short and intense X-ray pulses generated from XFELs, the initial steps of protein transitions can be directly visualized. Accordingly, fascinating opportunities are now available in the field of structural biology; that is, the entire structural dynamics of proteins in their physiological condition can be captured from beginning to end using TRXL at XFELs.

6. TIME-RESOLVED X-RAY LIQUIDOGRAPHY FOR SMALL MOLECULES

Although TRXL has lower structural resolution than TRXC, it can still reveal the atomic-level details of structural changes involved in chemical reactions of small molecules, unlike for macromolecules, because small molecules have much simpler molecular structures than macromolecules.

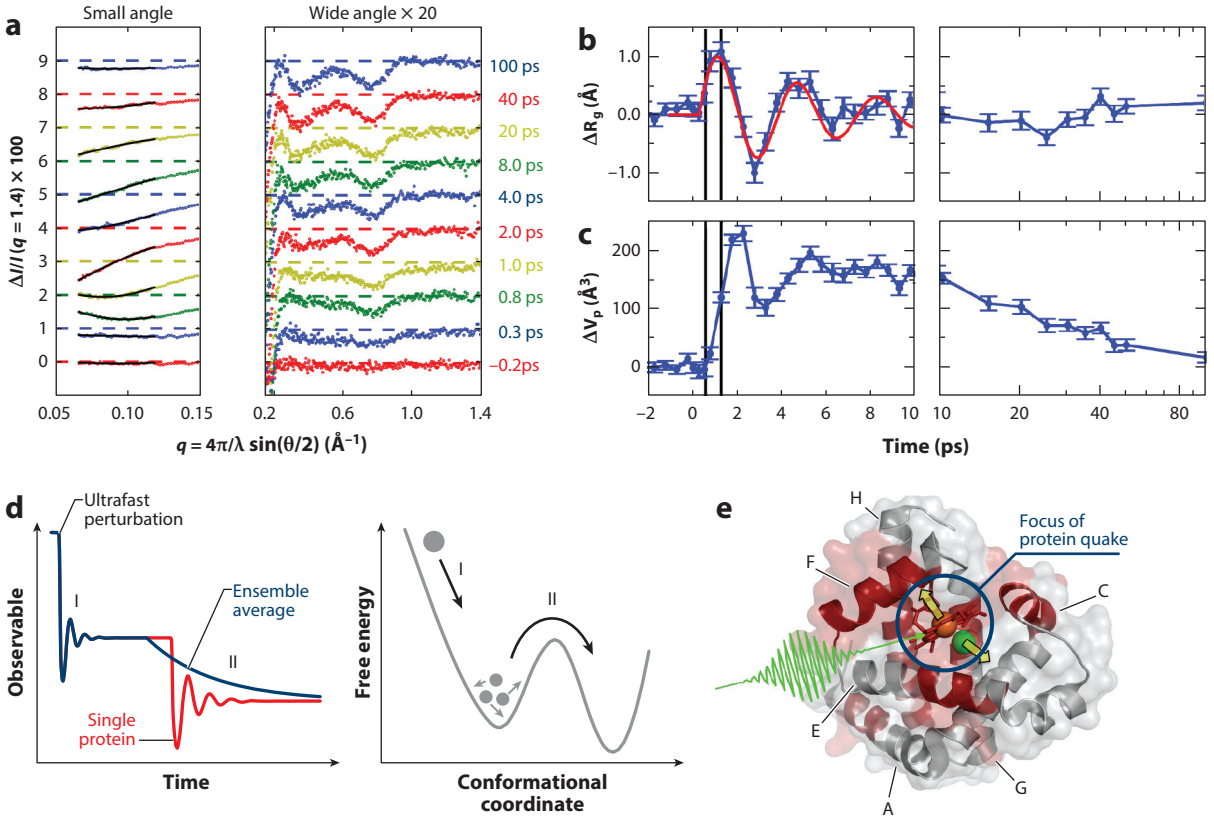

Figure 5

Ultrafast structural changes in CO-bound myoglobin (MbCO) observed by using time-resolved X-ray liquidography at an X-ray free-electron laser (119). (*a*) Time-resolved difference X-ray scattering intensities for MbCO in solution. The difference scattering intensities in both small-angle and wide-angle regions develop even before 1 ps, and their shape and amplitude change over time. The horizontal axis shows the magnitude q of the momentum transfer vector, represented as a function of the X-ray wavelength λ and the scattering angle θ. (*b*,*c*) Time-dependent changes of (*b*) the radius of gyration, R_g, and (*c*) the volume of the protein, V_p. Structural parameters of the protein can be obtained by Guinier analysis in the small-angle region (*black lines* in the small-angle curves in panel *a*). This analysis reveals that ultrafast increase of R_g by ∼1 Å occurs within 1 ps and is followed by delayed expansion of V_p by 220 Å^3 within 2 ps. In addition, it is clearly visualized that both R_g and V_p exhibit notable damped oscillations within 10 ps. (*d*) On the basis of observations of the oscillatory features, Cammarata and coworkers (119) postulated an intrinsic ballistic-like nature of the protein motion (*red curve*) that is generally hidden in ensemble measurements at longer timescales (*blue curve*). (*e*) Protein quake in MbCO. The segments exhibiting the collective oscillatory motions are highlighted in red. Abbreviations: SAXS, small-angle X-ray scattering; WAXS, wide-angle X-ray scattering.

In general, TRXL data for small molecules are analyzed by global fitting, in which the time-resolved difference scattering curves are fitted by theoretical scattering curves that are constructed by a linear combination of scattering curves calculated for all possible species involved in a reaction, that is, reactants, products, and intermediate species. From global fitting analysis, the identities of reactants, intermediates, and products, as well as their time-dependent concentrations, are obtained. In general, the molecular structures of chemical species used for calculating the theoretical scattering curves are obtained from quantum calculation. However, the exact structures of short-lived intermediate species are not known as well as the ground-state structures of reactants and products. Using TRXL, these structures can be determined more accurately by fitting the

time-resolved scattering curves while finely varying structural parameters of intermediates, such as bond lengths and bond angles. Besides the structural dynamics of solute molecules, collective motions of the solvation cage and solvent molecules can also be visualized by TRXL. This unique ability of probing the comprehensive structural dynamics of solution-phase reaction systems has made TRXL a powerful technique for studying reaction dynamics in solution.

Scattering from a solution sample is often dominated by scattering from numerous solvent molecules surrounding the solutes, especially for small solute molecules. However, when the solute contains strong scatterers such as halogen atoms and heavy metals, structural changes of even small solute molecules can be manifested as oscillatory features in the difference scattering curves. Accordingly, TRXL has mostly been used to investigate reaction dynamics of the following two classes of small molecules: halogen-containing organic molecules (126–132) and organometallic complexes containing heavy transition metals (133–142). Thus far, target systems studied by TRXL include molecular iodine (143), dihalogen and trihalogen molecules (143–148), haloalkanes (126–132), and coordination complexes (133–142).

The major shortcoming of TRXL experiments implemented at synchrotrons is their limited temporal resolution (∼100 ps), as was the case for TRXC as well. As a means of improving this limited temporal resolution, an experimental scheme called time slicing was developed (142, 145, 149). In the time-slicing scheme, time-resolved X-ray scattering curves at early time delays (for example, from −200 to 400 ps) are measured with fine steps (for example, 10 ps) that are much smaller than the temporal resolution of the experiment (∼100 ps). By deconvoluting the temporal profile of the X-ray pulse from the measured time-resolved difference scattering curves, the difference scattering curves, with less temporal blurring, can be retrieved at time delays shorter than 100 ps. In a TRXL study on geminate recombination of photoexcited molecular iodine (I_2), the time-slicing scheme was employed to visualize the formation of the vibrationally hot I_2 molecule, which has a longer I–I distance than the ground state, and its fast relaxation to the ground state (145). It should be noted that the vibrational relaxation occurs on the timescale of tens of picoseconds, which is not accessible without the time-slicing scheme. In the same work, collective motions of surrounding solvent molecules in response to the structural change of solute molecules were directly visualized, demonstrating the power of TRXL for resolving the complex solute–solvent interaction.

Many important elementary chemical reactions occur on ultrafast timescales from tens of femtoseconds to picoseconds, for example, the making and breaking of chemical bonds, isomerization, and charge transfer. The advent of XFELs provides the ability to probe the structural dynamics of such fast reactions in real time using TRXL. For example, the research group led by Ihee & Adachi (150, 151) visualized the bond formation process of a gold trimer complex, $[Au(CN)_2^-]_3$, in real time by performing TRXL at an XFEL (see **Figure 6**). Unlike for unimolecular processes such as bond breaking, it is difficult to precisely initiate and follow the diffusion-limited, bimolecular process of bond formation in solution with ultrahigh temporal resolution. The $[Au(CN)_2^-]_3$ trimer is a unique model system relevant for studying the bond formation process because gold atoms in this complex in the ground state are weakly bound to each other by noncovalent interaction (called aurophilicity) and, upon photoexcitation, covalent bonds are formed among the gold atoms without being limited by slow diffusion through the solvent. This study is the first example of probing the structural dynamics of a chemical reaction with subpicosecond temporal resolution using TRXL. In addition, anisotropic scattering patterns measured from transiently aligned molecules by linearly polarized photoexcitation were analyzed to obtain the rotational diffusion time (∼13 ps) of the gold trimer complex (152).

Haldrup and coworkers (153) recently studied the structural evolution of $[Co(terpy)_2]^{2+}$ [terpy = terpyridine or 2,6-bis(2-pyridyl) pyridine] complex triggered by a spin-state transition

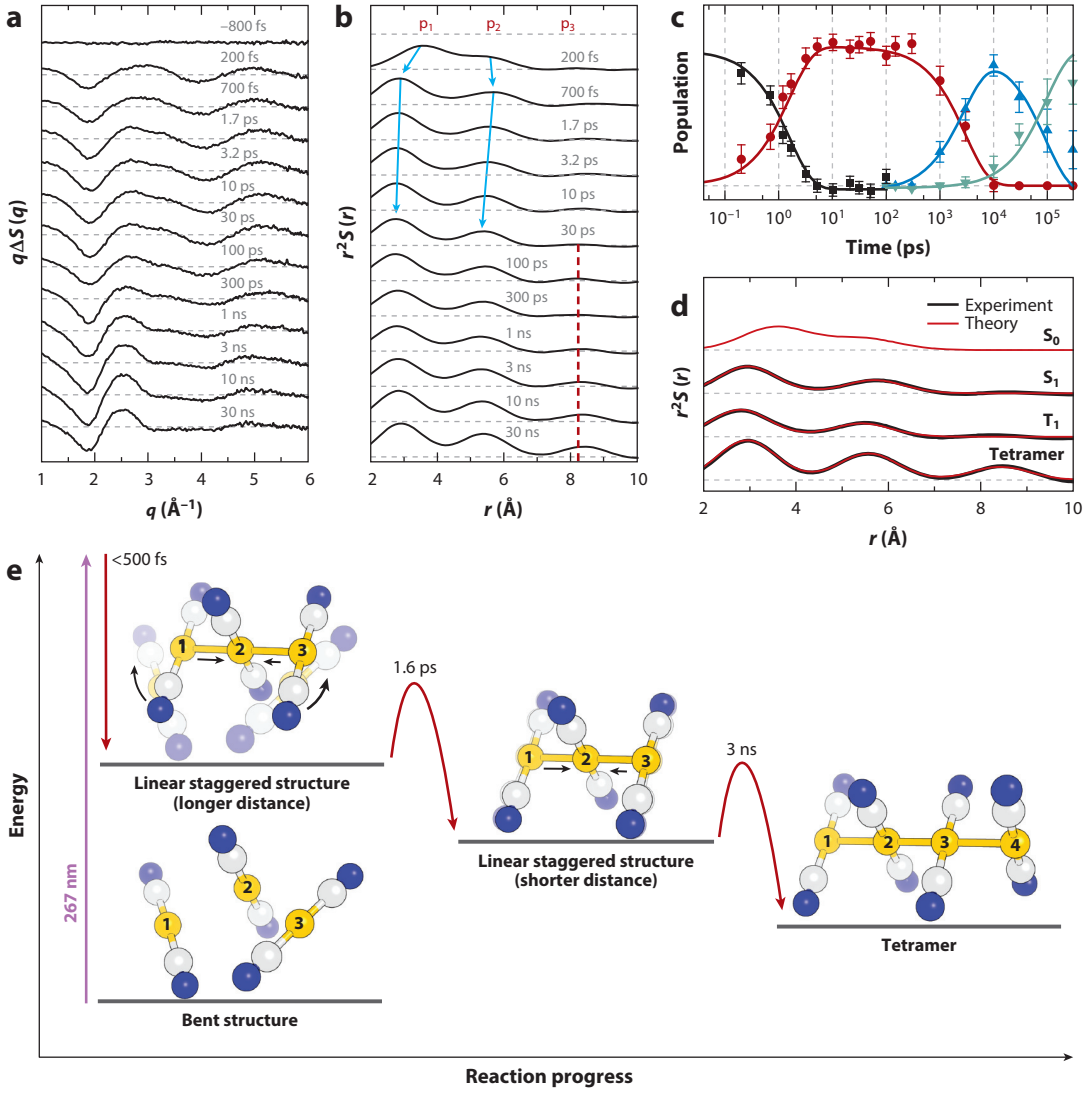

Figure 6

Photoinduced bond formation and related structural changes in $[Au(CN)_2^-]_3$ observed using time-resolved X-ray liquidography (TRXL) at an X-ray free-electron laser (150). (*a*) Experimental difference scattering curves as a function of the magnitude q of the momentum transfer vector measured at various time delays. (*b*) Radial distribution functions (RDFs) of transient species as a function of interatomic distance r at various time delays. The RDFs of transient species were obtained by adding the RDF of the ground state, S_0, to the difference RDFs, which were obtained by sine Fourier transformation of difference scattering curves after subtracting solvent contributions. The time-dependent change of the p_1 and p_2 peaks and the rise of the p_3 peak are emphasized by blue arrows and a red dashed line. The p_1 and p_2 peaks can be assigned to the distances between adjacent and distant Au atoms in the gold trimer, respectively, and the p_3 peak can be assigned to the longest distance between Au atoms in the gold tetramer. (*c*) Time-dependent concentrations of reaction intermediates (S_1, T_1, and tetramer) and the recovered ground state (S_0). (*d*) Species-associated RDFs of the ground state (S_0) and the intermediate species (S_1, T_1, and tetramer). The species-associated RDFs (*black*) were obtained from singular value decomposition and principal component analyses of the measured TRXL data, and their fits (*red*) were obtained by using model structures. (*e*) Mechanism of the photo-induced bond formation in $[Au(CN)_2^-]_3$. Upon photoexcitation, the gold trimer complex undergoes sequential structural changes, including covalent bond formation, bent-to-linear relaxation, Au–Au bond shortening, and tetramer formation. The structural dynamics associated with the formation of the Au–Au bond were visualized with subangstrom spatial resolution and subpicosecond temporal resolution.

using TRXL at an XFEL. In that study, it was revealed that the Co–N bond between the central metal atom and the surrounding ligands elongates with the formation of a high-spin state. Notably, the increase of Co–N bond length was followed by coherent oscillations of the bond length with small amplitude (~0.01 Å) and subpicosecond periods. The oscillations were interpreted to arise from impulsive vibronic excitation of two different vibrational modes of the complex, one a breathing-like mode and the other a pincer-like mode. This work is the first example of directly probing wave-packet dynamics in real space using time-resolved X-ray diffraction.

TRXGS: time-resolved X-ray gas scattering

Besides the works described above, several other investigations of small-molecule systems in the solution phase have been carried out by TRXL at XFELs to reveal interesting ultrafast phenomena, for example, ultrafast solvation dynamics of an iron complex (154) and nonequilibrium dynamics of intramolecular electron transfer in a bimetallic RuCo complex (155). These results demonstrate the unique capabilities of TRXL at XFELs, that is, it can (*a*) capture the ultrafast structural dynamics of chemical reactions in solution with subpicosecond temporal resolution and (*b*) elucidate the structural dynamics of solute, solvent, and solvation cage comprehensively.

7. CONCLUDING REMARKS

Owing to pioneering research efforts in the field of TRXC and TRXL, the methodologies of experiment and data analysis for those techniques are now well established and can be used to study a wide range of molecular reactions, from small molecules to macromolecules. In particular, with the advent of XFELs, it has become possible for TRXC and TRXL to access reaction dynamics on a subpicosecond timescale, where many important ultrafast processes in chemistry and biology occur. All we need to do is find out target systems of scientific importance, waiting for investigation using these methods. For example, the structural dynamics of molecules near conical intersections can be studied using TRXC or TRXL performed at an XFEL. Although the presence of conical intersections (156, 157) and the wave-packet dynamics near conical intersections (158, 159) have been intensively examined in energy space using spectroscopic tools (160), observation of the wave-packet motion in real space using time-resolved X-ray diffraction will be desirable to better understand the nonadiabatic behavior of excited molecules around conical intersections. For example, a recent TRXC study on PYP (58) showed that the ultrafast isomerization of the PYP chromophore occurs through a conical intersection.

Besides reactions in the crystalline and solution phases, chemical reactions in the gas phase can be explored by using time-resolved X-ray diffraction employing intense X-ray pulses from XFELs, that is, time-resolved X-ray gas scattering (TRXGS). In contrast to the condensed phase, the gas phase is an isolated, collision-free environment with negligible intermolecular interaction and thus is ideal for unambiguously elucidating reaction dynamics. In addition, the scattering data measured from gas-phase samples contain contributions only from target molecules of interest, making the data analysis simpler than for solution samples. Previously, TRXGS was not realized because of the low photon flux of X-ray pulses generated from synchrotrons, but a TRXGS experiment on the ring-opening reaction of 1,3-cyclohexadiene was recently demonstrated at an XFEL (161), giving a direct structural view of how the bond-breaking reaction occurs. This work clearly shows the feasibility of TRXGS experimentation at XFELs, opening a new opportunity for studies of chemical reaction dynamics in the gas phase.

Single-molecule X-ray scattering is another fascinating field that needs to be developed. Initially, the concept of single-molecule diffraction was proposed as a means of determining the 3D atomic structure of macromolecules without the need for crystallography (162), but later it was suggested that a single-shot, single-molecule scattering scheme might provide completely new opportunities for chemical reaction dynamics and biophysics (163, 164). For example, as

demonstrated from a theoretical study by Ihee and coworkers (164), a structural phase space spanned by structural fluctuation of molecules can be retrieved by single-object scattering sampling (SOSS) experiments. Such structural fluctuation is crucial to understanding the dynamic behavior of certain biomolecules, such as flexible proteins and RNAs. In addition, a state with extremely low population and short lifetime, for example the transition state of a chemical reaction, can be structurally characterized using SOSS experiments combined with time-resolved techniques. For experimental demonstrations, the biggest obstacle to the realization of SOSS experiments is recording single-shot, single-molecule scattering patterns with a sufficiently high SNR for structural analysis. The X-ray flux currently available from XFELs is still far from enough to produce strong scattering signals from most small molecules and biomolecules. Thus, a specially designed sample is required to amplify the single-shot, single-molecule scattering signal. The most straightforward method is to label the sample molecules with heavy scatterers such as gold nanoparticles in a site-specific manner.

SOSS: single-object scattering sampling

In this article, we have briefly reviewed the recent developments of time-resolved X-ray diffraction techniques and their applications to samples of various phases and sizes, with particular emphasis on experiments at XFELs. Although TRXC and TRXL performed at synchrotrons have already proven to be useful tools for probing the structural dynamics of chemical and biological processes, the recent development of XFELs has made them more powerful by extending their temporal resolution down to the femtosecond regime. In the near future, we are looking forward to more exciting and more scientifically valuable studies carried out using TRXC and TRXL methods at both synchrotrons and XFELs.

SUMMARY POINTS

1. Time-resolved X-ray diffraction provides a direct structural probe of dynamic processes by using a hard X-ray probe pulse in the pump–probe scheme and complements time-resolved optical spectroscopy.
2. Time-resolved X-ray diffraction is classified into time-resolved X-ray crystallography and time-resolved X-ray liquidography depending on the sample phase (single solid crystal versus liquid solution).
3. The temporal resolution of time-resolved X-ray diffraction is dictated by the temporal duration of X-ray pulses. X-ray pulses of 100-ps duration are generated from synchrotrons, whereas femtosecond X-ray pulses are available from recently developed X-ray free-electron lasers.
4. Serial femtosecond crystallography performed at X-ray free-electron lasers is a major breakthrough for time-resolved X-ray crystallography because it allows the use of small crystals as samples, minimizes radiation damage, achieves femtosecond temporal resolution, and is applicable to irreversible reactions.
5. Time-resolved X-ray liquidography can be used to elucidate comprehensive structural dynamics of chemical reactions and protein structural transitions in the solution phase, including the structural changes of solute, solvent, and solvation cage. In particular, time-resolved X-ray liquidography performed at X-ray free-electron lasers can probe ultrafast processes with femtosecond temporal resolution.

DISCLOSURE STATEMENT

The authors are not aware of any affiliations, memberships, funding, or financial holdings that might be perceived as affecting the objectivity of this review.

ACKNOWLEDGMENTS

This work was supported by IBS-R004-A1.

LITERATURE CITED

1. Moffat K. 1989. Time-resolved macromolecular crystallography. *Annu. Rev. Biophys. Biophys. Chem.* 18:309–32
2. Zewail AH. 2006. 4D ultrafast electron diffraction, crystallography, and microscopy. *Annu. Rev. Phys. Chem.* 57:65–103
3. Ihee H. 2009. Visualizing solution-phase reaction dynamics with time-resolved X-ray liquidography. *Acc. Chem. Res.* 42:356–66
4. Friedman JM, Rousseau DL, Ondrias MR. 1982. Time-resolved resonance Raman studies of hemoglobin. *Annu. Rev. Phys. Chem.* 33:471–91
5. Beechem JM, Brand L. 1985. Time-resolved fluorescence of proteins. *Annu. Rev. Biochem.* 54:43–71
6. Fleming GR. 1986. Subpicosecond spectroscopy. *Annu. Rev. Phys. Chem.* 37:81–104
7. Chen LX. 2005. Probing transient molecular structures in photochemical processes using laser-initiated time-resolved X-ray absorption spectroscopy. *Annu. Rev. Phys. Chem.* 56:221–54
8. Nibbering ETJ, Fidder H, Pines E. 2005. Ultrafast chemistry: using time-resolved vibrational spectroscopy for interrogation of structural dynamics. *Annu. Rev. Phys. Chem.* 56:337–67
9. Buckup T, Motzkus M. 2014. Multidimensional time-resolved spectroscopy of vibrational coherence in biopolyenes. *Annu. Rev. Phys. Chem.* 65:39–57
10. Pribram-Jones A, Gross DA, Burke K. 2015. DFT: a theory full of holes? *Annu. Rev. Phys. Chem.* 66:283–304
11. González L, Escudero D, Serrano-Andrés L. 2012. Progress and challenges in the calculation of electronic excited states. *ChemPhysChem* 13:28–51
12. Adamo C, Jacquemin D. 2013. The calculations of excited-state properties with time-dependent density functional theory. *Chem. Soc. Rev.* 42:845–56
13. Plech A, Kurbitz S, Berg KJ, Graener H, Berg G, et al. 2003. Time-resolved X-ray diffraction on laser-excited metal nanoparticles. *Europhys. Lett.* 61:762–68
14. Wagener P, Ibrahimkutty S, Menzel A, Plech A, Barcikowski S. 2013. Dynamics of silver nanoparticle formation and agglomeration inside the cavitation bubble after pulsed laser ablation in liquid. *Phys. Chem. Chem. Phys.* 15:3068–74
15. Jurgilaitis A, Enquist H, Andreasson BP, Persson AIH, Borg BM, et al. 2014. Time-resolved X-ray diffraction investigation of the modified phonon dispersion in InSb nanowires. *Nano Lett.* 14:541–46
16. Walko DA, Sheu YM, Trigo M, Reis DA. 2011. Thermal transport in thin films measured by time-resolved, grazing incidence X-ray diffraction. *J. Appl. Phys.* 110:102203
17. Puigdomenech J, Perezgrau L, Porta J, Vega MC, Sicre P, Koch MHJ. 1989. Time-resolved synchrotron radiation X-ray solution scattering study of DNA melting. *Biopolymers* 28:1505–14
18. Kendrew JC, Bodo G, Dintzis HM, Parrish RG, Wyckoff H, Phillips DC. 1958. A three-dimensional model of the myoglobin molecule obtained by X-ray analysis. *Nature* 181:662–66
19. Moffat K, Helliwell JR. 1989. The Laue method and its use in time-resolved crystallography. *Top. Curr. Chem.* 151:61–74
20. Gruner SM. 1987. Time-resolved X-ray diffraction of biological materials. *Science* 238:305–12
21. Schlichting I, Almo SC, Rapp G, Wilson K, Petratos K, et al. 1990. Time-resolved X-ray crystallographic study of the conformational change in Ha-Ras p21 protein on GTP hydrolysis. *Nature* 345:309–15
22. Hajdu J, Machin PA, Campbell JW, Greenhough TJ, Clifton IJ, et al. 1987. Millisecond X-ray diffraction and the first electron density map from Laue photographs of a protein crystal. *Nature* 329:178–81

23. Moffat K, Szebenyi D, Bilderback D. 1984. X-ray Laue diffraction from protein crystals. *Science* 223:1423–25
24. Golub GH, Reinsch C. 1970. Singular value decomposition and least squares solutions. *Numer. Math.* 14:403–20
25. Schmidt M, Rajagopal S, Ren Z, Moffat K. 2003. Application of singular value decomposition to the analysis of time-resolved macromolecular X-ray data. *Biophys. J.* 84:2112–29
26. Schmidt M, Pahl R, Srajer V, Anderson S, Ren Z, et al. 2004. Protein kinetics: structures of intermediates and reaction mechanism from time-resolved X-ray data. *PNAS* 101:4799–804
27. Ihee H, Rajagopal S, Srajer V, Pahl R, Anderson S, et al. 2005. Visualizing reaction pathways in photoactive yellow protein from nanoseconds to seconds. *PNAS* 102:7145–50
28. Rajagopal S, Anderson S, Srajer V, Schmidt M, Pahl R, Moffat K. 2005. A structural pathway for signaling in the E46Q mutant of photoactive yellow protein. *Structure* 13:55–63
29. Schmidt M, Nienhaus K, Pahl R, Krasselt A, Anderson S, et al. 2005. Ligand migration pathway and protein dynamics in myoglobin: a time-resolved crystallographic study on L29W MbCO. *PNAS* 102:11704–9
30. Key J, Srajer V, Pahl R, Moffat K. 2007. Time-resolved crystallographic studies of the heme domain of the oxygen sensor FixL: structural dynamics of ligand rebinding and their relation to signal transduction. *Biochemistry* 46:4706–15
31. Jung YO, Lee JH, Kim J, Schmidt M, Moffat K, et al. 2013. Volume-conserving *trans-cis* isomerization pathways in photoactive yellow protein visualized by picosecond X-ray crystallography. *Nat. Chem.* 5:212–20
32. Genick UK, Borgstahl GEO, Ng K, Ren Z, Pradervand C, et al. 1997. Structure of a protein photocycle intermediate by millisecond time-resolved crystallography. *Science* 275:1471–75
33. Perman B, Srajer V, Ren Z, Teng TY, Pradervand C, et al. 1998. Energy transduction on the nanosecond time scale: early structural events in a xanthopsin photocycle. *Science* 279:1946–50
34. Ren Z, Perman B, Srajer V, Teng TY, Pradervand C, et al. 2001. A molecular movie at 1.8 Å resolution displays the photocycle of photoactive yellow protein, a eubacterial blue-light receptor, from nanoseconds to seconds. *Biochemistry* 40:13788–801
35. Schotte F, Cho HS, Kaila VRI, Kamikubo H, Dashdorj N, et al. 2012. Watching a signaling protein function in real time via 100-ps time-resolved Laue crystallography. *PNAS* 109:19256–61
36. Knapp JE, Pahl R, Srajer V, Royer WE Jr. 2006. Allosteric action in real time: time-resolved crystallographic studies of a cooperative dimeric hemoglobin. *PNAS* 103:7649–54
37. Knapp JE, Pahl R, Cohen J, Nichols JC, Schulten K, et al. 2009. Ligand migration and cavities within Scapharca dimeric Hbl: studies by time-resolved crystallography, Xe binding, and computational analysis. *Structure* 17:1494–504
38. Srajer V, Teng TY, Ursby T, Pradervand C, Ren Z, et al. 1996. Photolysis of the carbon monoxide complex of myoglobin: nanosecond time-resolved crystallography. *Science* 274:1726–29
39. Srajer V, Ren Z, Teng TY, Schmidt M, Ursby T, et al. 2001. Protein conformational relaxation and ligand migration in myoglobin: a nanosecond to millisecond molecular movie from time-resolved Laue X-ray diffraction. *Biochemistry* 40:13802–15
40. Bourgeois D, Vallone B, Schotte F, Arcovito A, Miele AE, et al. 2003. Complex landscape of protein structural dynamics unveiled by nanosecond Laue crystallography. *PNAS* 100:8704–9
41. Schotte F, Lim MH, Jackson TA, Smirnov AV, Soman J, et al. 2003. Watching a protein as it functions with 150-ps time-resolved X-ray crystallography. *Science* 300:1944–47
42. Hummer G, Schotte F, Anfinrud PA. 2004. Unveiling functional protein motions with picosecond X-ray crystallography and molecular dynamics simulations. *PNAS* 101:15330–34
43. Bourgeois D, Vallone B, Arcovito A, Sciara G, Schotte F, et al. 2006. Extended subnanosecond structural dynamics of myoglobin revealed by Laue crystallography. *PNAS* 103:4924–29
44. Bourgeois D, Royant A. 2005. Advances in kinetic protein crystallography. *Curr. Opin. Struct. Biol.* 15:538–47
45. Westenhoff S, Nazarenko E, Malmerberg E, Davidsson J, Katona G, Neutze R. 2010. Time-resolved structural studies of protein reaction dynamics: a smorgasbord of X-ray approaches. *Acta Crystallogr. A* 66:207–19

46. Moffat K. 2014. Time-resolved crystallography and protein design: signalling photoreceptors and optogenetics. *Philos. Trans. R. Soc. B* 369:20130568
47. Chapman HN, Fromme P, Barty A, White TA, Kirian RA, et al. 2011. Femtosecond X-ray protein nanocrystallography. *Nature* 470:73–77
48. Spence JCH, Doak RB. 2004. Single molecule diffraction. *Phys. Rev. Lett.* 92:198102
49. Muniyappan S, Kim SO, Ihee H. 2015. Recent advances and future prospects of serial crystallography using XFEL and synchrotron X-ray sources. *Biodesign* 3:98–110
50. Schlichting I. 2015. Serial femtosecond crystallography: the first five years. *IUCrJ* 2:246–55
51. Neutze R, Wouts R, van der Spoel D, Weckert E, Hajdu J. 2000. Potential for biomolecular imaging with femtosecond X-ray pulses. *Nature* 406:752–57
52. Boutet S, Lomb L, Williams GJ, Barends TRM, Aquila A, et al. 2012. High-resolution protein structure determination by serial femtosecond crystallography. *Science* 337:362–64
53. Johansson LC, Arnlund D, Katona G, White TA, Barty A, et al. 2013. Structure of a photosynthetic reaction centre determined by serial femtosecond crystallography. *Nat. Commun.* 4:2911
54. Liu W, Wacker D, Gati C, Han GW, James D, et al. 2013. Serial femtosecond crystallography of G protein-coupled receptors. *Science* 342:1521–24
55. Redecke L, Nass K, DePonte DP, White TA, Rehders D, et al. 2013. Natively inhibited *Trypanosoma brucei* cathepsin B structure determined by using an X-ray laser. *Science* 339:227–30
56. Kern J, Alonso-Mori R, Tran R, Hattne J, Gildea RJ, et al. 2013. Simultaneous femtosecond X-ray spectroscopy and diffraction of photosystem II at room temperature. *Science* 340:491–95
57. Tenboer J, Basu S, Zatsepin N, Pande K, Milathianaki D, et al. 2014. Time-resolved serial crystallography captures high-resolution intermediates of photoactive yellow protein. *Science* 346:1242–46
58. Pande K, Hutchison CDM, Groenhof G, Aquila A, Robinson JS, et al. 2016. Femtosecond structural dynamics drives the *trans/cis* isomerization in photoactive yellow protein. *Science* 352:725–29
59. Kupitz C, Basu S, Grotjohann I, Fromme R, Zatsepin NA, et al. 2014. Serial time-resolved crystallography of photosystem II using a femtosecond X-ray laser. *Nature* 513:261–65
60. Aquila A, Hunter MS, Doak RB, Kirian RA, Fromme P, et al. 2012. Time-resolved protein nanocrystallography using an X-ray free-electron laser. *Opt. Express* 20:2706–16
61. Neutze R. 2014. Opportunities and challenges for time-resolved studies of protein structural dynamics at X-ray free-electron lasers. *Philos. Trans. R. Soc. B* 369:20130318
62. Mueller M, Jenni S, Ban N. 2007. Strategies for crystallization and structure determination of very large macromolecular assemblies. *Curr. Opin. Struct. Biol.* 17:572–79
63. Hunter MS, Fromme P. 2011. Toward structure determination using membrane-protein nanocrystals and microcrystals. *Methods* 55:387–404
64. Sugahara M, Mizohata E, Nango E, Suzuki M, Tanaka T, et al. 2015. Grease matrix as a versatile carrier of proteins for serial crystallography. *Nat. Methods* 12:61–63
65. Fromme P. 2015. XFELs open a new era in structural chemical biology. *Nat. Chem. Biol.* 11:895–99
66. Bostedt C, Boutet S, Fritz DM, Huang ZR, Lee HJ, et al. 2016. Linac coherent light source: the first five years. *Rev. Mod. Phys.* 88:015007
67. Barty A, Caleman C, Aquila A, Timneanu N, Lomb L, et al. 2012. Self-terminating diffraction gates femtosecond X-ray nanocrystallography measurements. *Nat. Photonics* 6:35–40
68. Yano J, Kern J, Irrgang KD, Latimer MJ, Bergmann U, et al. 2005. X-ray damage to the Mn_4Ca complex in single crystals of photosystem II: a case study for metalloprotein crystallography. *PNAS* 102:12047–52
69. Umena Y, Kawakami K, Shen JR, Kamiya N. 2011. Crystal structure of oxygen-evolving photosystem II at a resolution of 1.9 Å. *Nature* 473:55–60
70. Galstyan A, Robertazzi A, Knapp EW. 2012. Oxygen-evolving Mn cluster in photosystem II: the protonation pattern and oxidation state in the high-resolution crystal structure. *J. Am. Chem. Soc.* 134:7442–49
71. Suga M, Akita F, Hirata K, Ueno G, Murakami H, et al. 2015. Native structure of photosystem II at 1.95 Å resolution viewed by femtosecond X-ray pulses. *Nature* 517:99–103
72. Frauenfelder H, Sligar SG, Wolynes PG. 1991. The energy landscapes and motions of proteins. *Science* 254:1598–603

47. Demonstrates the first study using SFX to characterize the structure of macromolecules.

50. Provides a good review of the experimental approaches and the data analysis methods for SFX.

58. Demonstrates a femtosecond TRSFX study on the photoisomerization of photoactive yellow protein.

73. **Barends TRM, Foucar L, Ardevol A, Nass K, Aquila A, et al. 2015. Direct observation of ultrafast collective motions in CO myoglobin upon ligand dissociation. *Science* 350:445–50**
74. Stoddard BL, Koenigs P, Porter N, Petratos K, Petsko GA, Ringe D. 1991. Observation of the light-triggered binding of pyrone to chymotrypsin by Laue X-ray crystallography. *PNAS* 88:5503–7
75. Duke EMH, Wakatsuki S, Hadfield A, Johnson LN. 1994. Laue and monochromatic diffraction studies on catalysis in phosphorylase b crystals. *Protein Sci.* 3:1178–96
76. Stoddard BL, Cohen BE, Brubaker M, Mesecar AD, Koshland DE. 1998. Millisecond Laue structures of an enzyme-product complex using photocaged substrate analogs. *Nat. Struct. Mol. Biol.* 5:891–7
77. Schmidt M. 2013. Mix and inject: reaction initiation by diffusion for time-resolved macromolecular crystallography. *Adv. Cond. Matter Phys.* 2013:167276
78. Benedict JB, Makal A, Sokolow JD, Trzop E, Scheins S, et al. 2011. Time-resolved Laue diffraction of excited species at atomic resolution: 100 ps single-pulse diffraction of the excited state of the organometallic complex $Rh_2(\mu\text{-}PNP)_2(PNP)_2{\bullet}BPh_4$. *Chem. Commun.* 47:1704–6
79. Coppens P. 2011. Molecular excited-state structure by time-resolved pump-probe X-ray diffraction. What is new and what are the prospects for further progress? *J. Phys. Chem. Lett.* 2:616–21
80. Coppens P, Zheng SL, Gembicky M. 2008. Static and time-resolved photocrystallographic studies in supramolecular solids. *Z. Krist.* 223:265–71
81. Fullagar WK, Wu G, Kim C, Ribaud L, Sagerman G, Coppens P. 2000. Instrumentation for photocrystallographic experiments of transient species. *J. Synchrotron Rad.* 7:229–35
82. Kim CD, Pillet S, Wu G, Fullagar WK, Coppens P. 2002. Excited-state structure by time-resolved X-ray diffraction. *Acta Crystallogr. A* 58:133–37
83. Coppens P, Vorontsov II, Graber T, Kovalevsky AY, Chen YS, et al. 2004. Geometry changes of a Cu(I) phenanthroline complex on photoexcitation in a confining medium by time-resolved X-ray diffraction. *J. Am. Chem. Soc.* 126:5980–81
84. Vorontsov II, Graber T, Kovalevsky AY, Novozhilova IV, Gembicky M, et al. 2009. Capturing and analyzing the excited-state structure of a Cu(I) phenanthroline complex by time-resolved diffraction and theoretical calculations. *J. Am. Chem. Soc.* 131:6566–73
85. Vorontsov II, Kovalevsky AY, Chen YS, Graber T, Gembicky M, et al. 2005. Shedding light on the structure of a photoinduced transient excimer by time-resolved diffraction. *Phys. Rev. Lett.* 94:193003
86. Coppens P, Gerlits O, Vorontsov II, Kovalevsky AY, Chen YS, et al. 2004. A very large Rh–Rh bond shortening on excitation of the $[Rh_2(1,8\text{-diisocyano-}p\text{-menthane})_4]^{2+}$ ion by time-resolved synchrotron X-ray diffraction. *Chem. Commun.* 2004:2144–45
87. Lorenc M, Hebert J, Moisan N, Trzop E, Servol M, et al. 2009. Successive dynamical steps of photoinduced switching of a molecular Fe(III) spin-crossover material by time-resolved X-ray diffraction. *Phys. Rev. Lett.* 103:028301
88. Hoshino M, Uekusa H, Tomita A, Koshihara S, Sato T, et al. 2012. Determination of the structural features of a long-lived electron-transfer state of 9-mesityl-10-methylacridinium ion. *J. Am. Chem. Soc.* 134:4569–72
89. Coppens P, Pitak M, Gembicky M, Messerschmidt M, Scheins S, et al. 2009. The RATIO method for time-resolved Laue crystallography. *J. Synchrotron Radiat.* 16:226–30
90. Makal A, Trzop E, Sokolow J, Kalinowski J, Benedict J, Coppens P. 2011. The development of Laue techniques for single-pulse diffraction of chemical complexes: time-resolved Laue diffraction on a binuclear rhodium metal-organic complex. *Acta Crystallogr. A* 67:319–26
91. Collet E, Moisan N, Balde C, Bertoni R, Trzop E, et al. 2012. Ultrafast spin-state photoswitching in a crystal and slower consecutive processes investigated by femtosecond optical spectroscopy and picosecond X-ray diffraction. *Phys. Chem. Chem. Phys.* 14:6192–99
92. Jarzembska KN, Kaminski R, Fournier B, Trzop E, Sokolow JD, et al. 2014. Shedding light on the photochemistry of coinage-metal phosphorescent materials: a time-resolved Laue diffraction study of an Ag^{I}-Cu^{I} tetranuclear complex. *Inorg. Chem.* 53:10594–601
93. Makal A, Benedict J, Trzop E, Sokolow J, Fournier B, et al. 2012. Restricted photochemistry in the molecular solid state: structural changes on photoexcitation of Cu(I) phenanthroline metal-to-ligand charge transfer (MLCT) complexes by time-resolved diffraction. *J. Phys. Chem. A* 116:3359–65

73. Demonstrates the first femtosecond TRSFX study.

94. Coppens P, Fournier B. 2015. New methods in time-resolved Laue pump-probe crystallography at synchrotron sources. *J. Synchrotron Radiat.* 22:280–7

95. Gao M, Lu C, Jean-Ruel H, Liu LC, Marx A, et al. 2013. Mapping molecular motions leading to charge delocalization with ultrabright electrons. *Nature* 496:343–46

96. Jean-Ruel H, Gao M, Kochman MA, Lu C, Liu LC, et al. 2013. Ring-closing reaction in diarylethene captured by femtosecond electron crystallography. *J. Phys. Chem. B* 117:15894–902

97. Kim KH, Muniyappan S, Oang KY, Kim JG, Nozawa S, et al. 2012. Direct observation of cooperative protein structural dynamics of homodimeric hemoglobin from 100 ps to 10 ms with pump-probe X-ray solution scattering. *J. Am. Chem. Soc.* 134:7001–8

98. Arnlund D, Johansson LC, Wickstrand C, Barty A, Williams GJ, et al. 2014. Visualizing a protein quake with time-resolved X-ray scattering at a free-electron laser. *Nat. Methods* 11:923–26

99. Takala H, Bjorling A, Berntsson O, Lehtivuori H, Niebling S, et al. 2014. Signal amplification and transduction in phytochrome photosensors. *Nature* 509:245–48

100. Kim TW, Lee JH, Choi J, Kim KH, van Wilderen LJ, et al. 2012. Protein structural dynamics of photoactive yellow protein in solution revealed by pump-probe X-ray solution scattering. *J. Am. Chem. Soc.* 134:3145–53

101. Kim TW, Kim JG, Yang C, Ki H, Jo J, Ihee H. 2014. Pump-probe X-ray solution scattering reveals accelerated folding of cytochrome upon suppression of misligation. *Bull. Korean Chem. Soc.* 35:695–96

102. Oang KY, Kim JG, Yang C, Kim TW, Kim Y, et al. 2014. Conformational substates of myoglobin intermediate resolved by picosecond X-ray solution scattering. *J. Phys. Chem. Lett.* 5:804–8

103. Oang KY, Kim KH, Jo J, Kim YM, Kim JG, et al. 2014. Sub-100-ps structural dynamics of horse heart myoglobin probed by time-resolved X-ray solution scattering. *Chem. Phys.* 442:137–42

104. Kim JG, Muniyappan S, Oang KY, Kim TW, Yang C, et al. 2016. Cooperative protein structural dynamics of homodimeric hemoglobin linked to water cluster at subunit interface revealed by time-resolved X-ray solution scattering. *Struct. Dyn.* 3:023610

105. Ihee H, Wulff M, Kim J, Adachi S. 2010. Ultrafast X-ray scattering: structural dynamics from diatomic to protein molecules. *Int. Rev. Phys. Chem.* 29:453–520

106. Kim TK, Lee JH, Wulff M, Kong QY, Ihee H. 2009. Spatiotemporal kinetics in solution studied by time-resolved X-ray liquidography (solution scattering). *ChemPhysChem* 10:1958–80

107. Kim J, Kim KH, Oang KY, Lee JH, Hong K, et al. 2016. Tracking reaction dynamics in solution by pump-probe X-ray absorption spectroscopy and X-ray liquidography (solution scattering). *Chem. Commun.* 52:3734–49

108. Kim KH, Kim J, Lee JH, Ihee H. 2014. Molecular reaction and solvation visualized by time-resolved X-ray solution scattering: structure, dynamics, and their solvent dependence. *Struct. Dyn.* 1:011301

109. Kim JG, Kim TW, Kim J, Ihee H. 2015. Protein structural dynamics revealed by time-resolved X-ray solution scattering. *Acc. Chem. Res.* 48:2200–8

110. Cammarata M, Levantino M, Schotte F, Anfinrud PA, Ewald F, et al. 2008. Tracking the structural dynamics of proteins in solution using time-resolved wide-angle X-ray scattering. *Nat. Methods* 5:881–86

111. Ahn S, Kim KH, Kim Y, Kim J, Ihee H. 2009. Protein tertiary structural changes visualized by time-resolved X-ray solution scattering. *J. Phys. Chem. B* 113:13131–33

112. Cho HS, Dashdorj N, Schotte F, Graber T, Henning R, Anfinrud P. 2010. Protein structural dynamics in solution unveiled via 100-ps time-resolved X-ray scattering. *PNAS* 107:7281–86

113. Kim KH, Oang KY, Kim J, Lee JH, Kim Y, Ihee H. 2011. Direct observation of myoglobin structural dynamics from 100 picoseconds to 1 microsecond with picosecond X-ray solution scattering. *Chem. Commun.* 47:289–91

114. Kim J, Kim KH, Kim JG, Kim TW, Kim Y, Ihee H. 2011. Anisotropic picosecond X-ray solution scattering from photoselectively aligned protein molecules. *J. Phys. Chem. Lett.* 2:350–56

115. Andersson M, Malmerberg E, Westenhoff S, Katona G, Cammarata M, et al. 2009. Structural dynamics of light-driven proton pumps. *Structure* 17:1265–75

116. Kim TW, Yang C, Kim Y, Kim JG, Kim J, et al. 2016. Combined probes of X-ray scattering and optical spectroscopy reveal how global conformational change is temporally and spatially linked to local structural perturbation in photoactive yellow protein. *Phys. Chem. Chem. Phys.* 18:8911–19

94. Provides a good review of the data analysis method for TRXC studies of molecular crystals.

98. Presents the first femtosecond TRXL study on macromolecules performed at an XFEL.

108. Provides a good review of the TRXL studies on small molecules at synchrotrons.

109. Provides a good review of the TRXL studies on macromolecules at synchrotrons.

117. Ramachandran PL, Lovett JE, Carl PJ, Cammarata M, Lee JH, et al. 2011. The short-lived signaling state of the photoactive yellow protein photoreceptor revealed by combined structural probes. *J. Am. Chem. Soc.* 133:9395–404
118. Kikhney AG, Svergun DI. 2015. A practical guide to small angle X-ray scattering (SAXS) of flexible and intrinsically disordered proteins. *FEBS Lett.* 589:2570–77
119. Levantino M, Schiro G, Lemke HT, Cottone G, Glownia JM, et al. 2015. Ultrafast myoglobin structural dynamics observed with an X-ray free-electron laser. *Nat. Commun.* 6:6772
120. Vos MH, Rappaport F, Lambry JC, Breton J, Martin JL. 1993. Visualization of coherent nuclear motion in a membrane protein by femtosecond spectroscopy. *Nature* 363:320–25
121. Rischel C, Spiedel D, Ridge JP, Jones MR, Breton J, et al. 1998. Low frequency vibrational modes in proteins: changes induced by point-mutations in the protein-cofactor matrix of bacterial reaction centers. *PNAS* 95:12306–11
122. Wang HY, Lin S, Allen JP, Williams JC, Blankert S, et al. 2007. Protein dynamics control the kinetics of initial electron transfer in photosynthesis. *Science* 316:747–50
123. Wang HY, Lin S, Katilius E, Laser C, Allen JP, et al. 2009. Unusual temperature dependence of photosynthetic electron transfer due to protein dynamics. *J. Phys. Chem. B* 113:818–24
124. Ansari A, Berendzen J, Bowne SF, Frauenfelder H, Iben IE, et al. 1985. Protein states and proteinquakes. *PNAS* 82:5000–4
125. Miyashita O, Onuchic JN, Wolynes PG. 2003. Nonlinear elasticity, proteinquakes, and the energy landscapes of functional transitions in proteins. *PNAS* 100:12570–75
126. Neutze R, Wouts R, Techert S, Davidsson J, Kocsis M, et al. 2001. Visualizing photochemical dynamics in solution through picosecond X-ray scattering. *Phys. Rev. Lett.* 87:195508
127. Davidsson J, Poulsen J, Cammarata M, Georgiou P, Wouts R, et al. 2005. Structural determination of a transient isomer of CH_2I_2 by picosecond X-ray diffraction. *Phys. Rev. Lett.* 94:245503
128. Ihee H, Lorenc M, Kim TK, Kong QY, Cammarata M, et al. 2005. Ultrafast X-ray diffraction of transient molecular structures in solution. *Science* 309:1223–27
129. Kong QY, Wulff M, Lee JH, Bratos S, Ihee H. 2007. Photochemical reaction pathways of carbon tetrabromide in solution probed by picosecond X-ray diffraction. *J. Am. Chem. Soc.* 129:13584–91
130. Lee JH, Kim J, Cammarata M, Kong Q, Kim KH, et al. 2008. Transient X-ray diffraction reveals global and major reaction pathways for the photolysis of iodoform in solution. *Angew. Chem. Int. Ed.* 47:1047–50
131. Lee JH, Kim TK, Kim J, Kong Q, Cammarata M, et al. 2008. Capturing transient structures in the elimination reaction of haloalkane in solution by transient X-ray diffraction. *J. Am. Chem. Soc.* 130:5834–35
132. Kim J, Lee JH, Kim J, Jun S, King KH, et al. 2012. Structural dynamics of 1,2-diiodoethane in cyclohexane probed by picosecond X-ray liquidography. *J. Phys. Chem. A* 116:2713–22
133. Kim TK, Lorenc M, Lee JH, Russo M, Kim J, et al. 2006. Spatiotemporal reaction kinetics of an ultrafast photoreaction pathway visualized by time-resolved liquid X-ray diffraction. *PNAS* 103:9410–15
134. Kong QY, Lee JH, Plech A, Wulff M, Ihee H, Koch MHJ. 2008. Ultrafast X-ray solution scattering reveals an unknown reaction intermediate in the photolysis of $[Ru_3(CO)_{12}]$. *Angew. Chem. Int. Ed.* 47:5550–53
135. Christensen M, Haldrup K, Bechgaard K, Feidenhans'l R, Kong QY, et al. 2009. Time-resolved X-ray scattering of an electronically excited state in solution. Structure of the $^3A_{2u}$ state of tetrakis-μ-pyrophosphitodiplatinate(II). *J. Am. Chem. Soc.* 131:502–8
136. Jun S, Lee JH, Kim J, Kim J, Kim KH, et al. 2010. Photochemistry of $HgBr_2$ in methanol investigated using time-resolved X-ray liquidography. *Phys. Chem. Chem. Phys.* 12:11536–47
137. Kong Q, Lee JH, Kim KH, Kim J, Wulff M, et al. 2010. Ultrafast X-ray solution scattering reveals different reaction pathways in the photolysis of triruthenium dodecacarbonyl ($Ru_3(CO)_{12}$) after ultraviolet and visible excitation. *J. Am. Chem. Soc.* 132:2600–7
138. Christensen M, Haldrup K, Kjaer KS, Cammarata M, Wulff M, et al. 2010. Structure of a short-lived excited state trinuclear Ag–Pt–Pt complex in aqueous solution by time resolved X-ray scattering. *Phys. Chem. Chem. Phys.* 12:6921–23

119. Presents the femtosecond TRXL study on the ligand photodissociation of CO myoglobin.

139. Vanko G, Bordage A, Papai M, Haldrup K, Gatzel P, et al. 2015. Detailed characterization of a nanosecond-lived excited state: X-ray and theoretical investigation of the quintet state in photoexcited $[Fe(terpy)_2]^{2+}$. *J. Phys. Chem. C* 119:5888–902
140. Haldrup K, Christensen M, Nielsen MM. 2010. Analysis of time-resolved X-ray scattering data from solution-state systems. *Acta Crystallogr. A* 66:261–69
141. Haldrup K, Vanko G, Gawelda W, Galler A, Doumy G, et al. 2012. Guest–host interactions investigated by time-resolved X-ray spectroscopies and scattering at MHz rates: solvation dynamics and photoinduced spin transition in aqueous $Fe(bipy)_3{}^{2+}$. *J. Phys. Chem. A* 116:9878–87
142. Haldrup K, Harlang T, Christensen M, Dohn A, van Driel TB, et al. 2011. Bond shortening (1.4 Å) in the singlet and triplet excited states of $[Ir_2(dimen)_4]^{2+}$ in solution determined by time-resolved X-ray scattering. *Inorg. Chem.* 50:9329–36
143. Plech A, Wulff M, Bratos S, Mirloup F, Vuilleumier R, et al. 2004. Visualizing chemical reactions in solution by picosecond X-ray diffraction. *Phys. Rev. Lett.* 92:125505
144. Kim KH, Lee JH, Kim J, Nozawa S, Sato T, et al. 2013. Solvent-dependent molecular structure of ionic species directly measured by ultrafast X-ray solution scattering. *Phys. Rev. Lett.* 110:165505
145. Lee JH, Wulff M, Bratos S, Petersen J, Guerin L, et al. 2013. Filming the birth of molecules and accompanying solvent rearrangement. *J. Am. Chem. Soc.* 135:3255–61
146. Kim KH, Ki H, Lee JH, Park S, Kong Q, et al. 2015. Solvent-dependent structure of molecular iodine probed by picosecond X-ray solution scattering. *Phys. Chem. Chem. Phys.* 17:8633–37
147. Kong QY, Lee JH, Lo Russo M, Kim TK, Lorenc M, et al. 2010. Photolysis of Br_2 in CCl_4 studied by time-resolved X-ray scattering. *Acta Crystallogr. A* 66:252–60
148. Wulff M, Bratos S, Plech A, Vuilleumier R, Mirloup F, et al. 2006. Recombination of photodissociated iodine: a time-resolved X-ray-diffraction study. *J. Chem. Phys.* 124:034501
149. Neutze R, Wouts R. 2000. Deconvoluting ultrafast structural dynamics: temporal resolution beyond the pulse length of synchrotron radiation. *J. Synchrotron Radiat.* 7:22–26

150. Presents the first successful femtosecond TRXL study on small molecules performed at an XFEL.

150. Kim KH, Kim JG, Nozawa S, Sato T, Oang KY, et al. 2015. Direct observation of bond formation in solution with femtosecond X-ray scattering. *Nature* 518:385–89

151. Kim KH, Kim JG, Oang KY, Kim TW, Ki H, et al. 2016. Femtosecond X-ray solution scattering reveals that bond formation mechanism of a gold trimer complex is independent of excitation wavelength. *Struct. Dyn.* 3:043209
152. Kim JG, Kim KH, Oang KY, Kim TW, Ki H, et al. 2015. Rotational dephasing of a gold complex probed by anisotropic femtosecond X-ray solution scattering using an X-ray free-electron laser. *J. Phys. B* 48:244005

153. Presents the femtosecond TRXL study on the spin-state transition of a Co complex performed at an XFEL.

153. Biasin E, van Driel TB, Kjaer KS, Dohn AO, Christensen M, et al. 2016. Femtosecond X-ray scattering study of ultrafast photoinduced structural dynamics in solvated $[Co(terpy)_2]^{2+}$. *Phys. Rev. Lett.* 117:013002

154. Haldrup K, Gawelda W, Abela R, Alonso-Mori R, Bergmann U, et al. 2016. Observing solvation dynamics with simultaneous femtosecond X-ray emission spectroscopy and X-ray scattering. *J. Phys. Chem. B* 120:1158–68
155. Canton SE, Kjaer KS, Vanko G, van Driel TB, Adachi SI, et al. 2015. Visualizing the non-equilibrium dynamics of photoinduced intramolecular electron transfer with femtosecond X-ray pulses. *Nat. Commun.* 6:6359
156. Han S, You HS, Kim SY, Kim SK. 2014. Dynamic role of the intramolecular hydrogen bonding in nonadiabatic chemistry revealed in the UV photodissociation reactions of 2-fluorothiophenol and 2-chlorothiophenol. *J. Phys. Chem. A* 118:6940–49
157. You HS, Han S, Yoon JH, Lim JS, Lee J, et al. 2015. Structure and dynamic role of conical intersections in the $\pi\sigma^*$-mediated photodissociation reactions. *Int. Rev. Phys. Chem.* 34:429–59
158. Lim JS, Kim SK. 2010. Experimental probing of conical intersection dynamics in the photodissociation of thioanisole. *Nat. Chem.* 2:627–32
159. Polli D, Altoè P, Weingart O, Spillane KM, Manzoni C, et al. 2010. Conical intersection dynamics of the primary photoisomerization event in vision. *Nature* 467:440–43
160. Domcke W, Yarkony DR. 2012. Role of conical intersections in molecular spectroscopy and photoinduced chemical dynamics. *Annu. Rev. Phys. Chem.* 63:325–52

161. Minitti MP, Budarz JM, Kirrander A, Robinson JS, Ratner D, et al. 2015. Imaging molecular motion: femtosecond X-ray scattering of an electrocyclic chemical reaction. *Phys. Rev. Lett.* 114:255501
162. Hajdu J. 2000. Single-molecule X-ray diffraction. *Curr. Opin. Struct. Biol.* 10:569–73
163. Ihee H. 2011. Novel single-molecule technique by single-object scattering sampling (SOSS). *Bull. Korean Chem. Soc.* 32:1849–50
164. Ki H, Kim KH, Kim J, Lee JH, Kim J, Ihee H. 2013. Prospect of retrieving vibrational wave function by single-object scattering sampling. *J. Phys. Chem. Lett.* 4:3345–50
165. Busse G, Tschentscher T, Plech A, Wulff M, Frederichs B, Techert S. 2003. First investigations of the kinetics of the topochemical reaction of *p*-formyl-*trans*-cinnamic acid by time-resolved X-ray diffraction. *Faraday Discuss.* 122:105–17

Annual Review of
Physical Chemistry
Volume 68, 2017

Contents

Indexes

Errata

An online log of corrections to *Annual Review of Physical Chemistry* articles may be found at http://www.annualreviews.org/errata/physchem